

MUSTANSIRIYAH JOURNAL OF PURE AND APPLIED SCIENCES

Journal homepage:

https://mjpas.uomustansiriyah.edu.iq/index.php/mjpas



RESEARCH ARTICLE - PHYSICS

Effect of the optical filter on the chaotic behavior of an optical artificial neuron

Mustafa M. Jaber^{1,2*} and Ayser A. Hemed¹

¹Department of Physics, College of Education, Mustansiriyah University, Baghdad, Iraq ²Resafa Directorate of Education, Baghdad, Iraq

*Corresponding author. E-mail: mostafajaber@uomustansiriyah.edu.iq.

Article Info.	Abstract
Article history:	The operation of an optical neural network via feed-forward (FF) configuration is experimentally simulated in the laboratory. The FF setup is tested using optical injection (OI),
Received	and the behavior of follower laser diodes (FLDs) subjected to chaotic modulation is examined.
5 August 2024	The last two laser diodes (LDs) are exposed to different weights of chaotic modulated signals
Accepted 2 September 2024	through optical filtration and attenuation. Observations of the emissions from these two FLDs during FF operation are verified by frequency spectra calculated from time series data. Signal
Publishing 30 September 2025	broadening is assessed by measuring the full width at half maximum (FWHM), and chaotic signal spikes are analyzed by counting the number of peaks associated with signal amplitudes for the FLDs. Additionally, LD control parameters, including the bias voltage of the influencer laser diodes (ILD1, ILD2) and two additional FLDs, are examined. A maximum FWHM of
	1.25 GHz for FLD2 is observed with a bias voltage of 3.6V and a modulated signal attenuation
	of -12dB. To determine the synchronization state, the correlation between the ILDs and FLDs
	is calculated. Results indicate fluctuations between negative and positive values, with the best
	correlation value being 0.4. These results confirm anti-synchronized ILD-FLDs, which is
	crucial for ensuring privacy in transmitting units within a chaotic optical communication
	system simulating an optical neural network.

This is an open-access article under the CC BY 4.0 license (http://creativecommons.org/licenses/by/4.0/)

The official journal published by the College of Education at Mustansiriya University

Keywords: Chaos, Adaline, neural networks, feed-for-word, optical communication.

1. Introduction

Optical injection is a technique for synchronizing optical phase and frequency through photonphoton interactions when external light enters a laser cavity[1,2]. In this system, a "master" laser provides external seed light to influence a "slave" laser. The master laser is coupled to the slave laser via a circulator or isolator to prevent stray reflections back to the master laser. When the carrier frequency (wavelength) of the master laser is close to that of the slave laser, the slave laser synchronizes with the master laser, emitting a laser with a constant phase shift at the same frequency. Additionally, the slave laser tracks any slow frequency drift of the master laser, maintaining a relatively constant power output. Laser synchronization is crucial in various applications. In optical communications, synchronized lasers serve as local oscillators (LOs) to reduce complexity and latency in coherent receivers[3,4].

The rate equations of the master and slave lasers can be expressed as [5]:

Master laser

$$\frac{dE_m(t)}{dt} = \frac{\alpha}{2} G_N [N_m - N_{th}] E_m(t) \tag{1}$$

$$\frac{d\phi_m(t)}{dt} = \frac{1}{2} G_N [N_m - N_{th}] \tag{2}$$

$$\frac{dN_m(t)}{dt} = J_m - \frac{N_m(t)}{\tau_s} - G_N [N_m - N_o] E^2_m(t) \tag{3}$$

$$\frac{d\theta_m(t)}{dt} = \frac{1}{2}G_N[N_m - N_{th}] \tag{2}$$

$$\frac{dN_m(t)}{dt} = J_m - \frac{N_m(t)}{\tau_c} - G_N[N_m - N_o]E^2_m(t)$$
 (3)

Slave laser:

$$\frac{dE_{sl}(t)}{dt} = \frac{\alpha}{2} G_N [N_{sl} - N_{th}] E_{sl}(t) + \frac{k_{in}}{\tau_{in}} E_{in}(t) \cos[\psi(t)]$$
 (4)

$$\frac{d\emptyset_{sl}(t)}{dt} = \frac{1}{2}G_N[N_{sl} - N_{th}] - \frac{k_{in}}{\tau_{in}}\frac{E_{in}}{E_m}(t)\sin[\psi(t)]$$

$$\frac{dN_{sl}(t)}{dt} = J_{sl} - \frac{N_{sl}(t)}{\tau_s} - G_N[N_{sl} - N_o]E^2_{sl}(t)$$
(6)

$$\frac{dN_{sl}(t)}{dt} = J_{sl} - \frac{N_{sl}(t)}{\tau_c} - G_N[N_{sl} - N_o]E^2_{sl}(t)$$
 (6)

$$\psi(t) = \emptyset_m - \emptyset_{sl} - \Delta wt \tag{7}$$

where:

E(t): is the amplitude of the electric field.

 \emptyset (t): is the phase of the electric field.

GN: is the modal gain. N(t): is the carrier density.

Nth: is the threshold carrier density. α : is the linewidth enhancement factor. τ_{in} : is the intracavity roundtrip time.

 τ_s ; is the carrier lifetime.

J: is injection current density.

k_{inj}: is the injection coefficient.

E_{ini}: is the injected electric field and is equal to the output.

 E_m : electric field of the master laser diode.

 ϕ_m , ϕ_{sl} : is the angular frequency detuning between the angular frequencies of master and slave laser diodes.

Because it can reduce distortion in all orders of magnitude and provide broadband distortion reduction at high frequencies, feed-forward linearization is a useful technique for laser nonlinearity compensation systems, irrespective of the nonlinear characteristics of the laser. But because feedforward entails canceling two signals that are almost equivalent in size and phase, it is also a delicate and complex technique [6,7]. Because it requires two lasers with very comparable distortion qualities, quasi-feed forward is challenging to execute. Predistortion often only significantly reduces distortion in modulators [8,9]. Initially, based on the theory of artificial neural networks, they explain the foundations of an optical matrix multiplier for linear operation in optical neural network development. Then, the optical neural network produced by free-space and waveguide optical connections is presented [10, 11].

The advantages of optical devices over electrical ones are leveraged by optical networks. For example, data can be transported from a single point source to any number of recipients, whereas doing the same with electronics would require a large volume of cables [13]. The human physiological system's time-delay mechanisms are essential for controlling the production of white blood cells and respiration rate. A neural network is an input-output system made up of many simple processing elements that share common characteristics. Every processing element has a number of internal variables known as "weights." Changing one element's weight will alter that element's behavior, which will alter the behavior of the entire network[14]. An optical neural network (ONN), is made up of several interconnected linear layers. In biological networks, individual neurons are triggered by presynaptic currents from neighboring neurons as well as any external currents that may be present [10]. ANNs emulate brain activity by simulating a collection of interconnected neurons, arranged in layers. The simplest representation will have three layers: an input layer, an output layer, and a hidden layer in between these two layers figure (1). The input layer accepts data from outside the ANN; the hidden layer is where the computation happens; and the output layer is where we can get the results from the neural network. The activation functions also play an important part in simulating intelligence. Mathematically, without appropriate activation functions, the neuron model is a simple linear model, which multiplies and accumulates input-weight products [16].

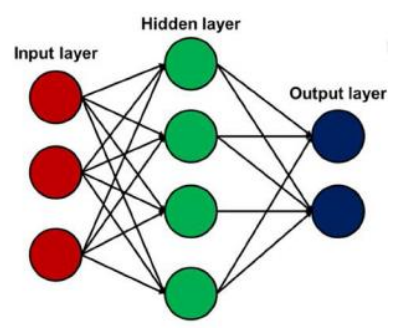


Fig. 1. Feed-forward artificial neural network [16].

It has been shown that the memristive neuron and neural network models can generate complex chaotic behaviors. For example, for the first time, chaotic spiking spiking and bursting firings are observed in memristive HR neurons [16,17]. The phenomena of chaos and synchronization is obtained in memristive bi-neuron networks [18,19,20,21]. Various complex chaotic phenomena including hyperchaos [22,23], hidden attractors [24,25,26], coexisting attractors [27,28], and multiscroll attractors [29,30] are discovered in various memristive neurons and neural networks. Also, the complicated dynamics of multistability [31,32], and extreme multistability [33,34], have been reported. Besides, the memristive neuron and neural network models owning complex dynamics can be better applied in artificial intelligence fields, especially secure communication [36]. Our work aims at first to verify the practical simulation of the optical artificial neuron algorithm and the use of the concept of chaos by optical pumping method through it and then to study the control of chaos by optical attenuation of the effective laser power and its effect on the chaos of the follower laser.

2. Experimental setup

Figure 2 illustrates our optical neural network setup, consisting of two neural ILD lasers (inputs) injecting two neural FLD lasers (hidden). In our setup, a continuous-wave (CW) laser diode, designated as the influencer laser diode (ILD) with the commercial code HFCT5205 uses a multiquantum well laser, operates at a wavelength of 1310 nm with a maximum power output of 0.1 mW. The ILD directs its output toward a variable optical fiber attenuator (OFA) and then to a fiber optical circulator (OC), with the reflected port being blocked. The transmission port is connected to a uniform fiber Bragg grating (UFBG1), commercially coded as SMF-28E, with a Bragg wavelength λB =1310.36 nm and a reflectivity of 84%. After passing through UFBG1, the signal goes through a 1×2 optical fiber splitter (OFS), dividing the emitted light into two parts with a measured splitting ratio of 10:90%. The 10% branch is detected by a photodetector (PD) integrated into the same HFCT5205 device. The remaining laser branch is routed through an optical isolator (OI) to block any back reflections. The filtered signal is then split into two by a 50% optical splitter. One part is injected into the follower laser diode (FLD) in the first branch, while the other part is directed to inject the FLD in the second branch. The same procedure is followed in the second branch, with a modification in the UFBG to λB =1310.23. Finally, a coupler is used to sum the two signals.

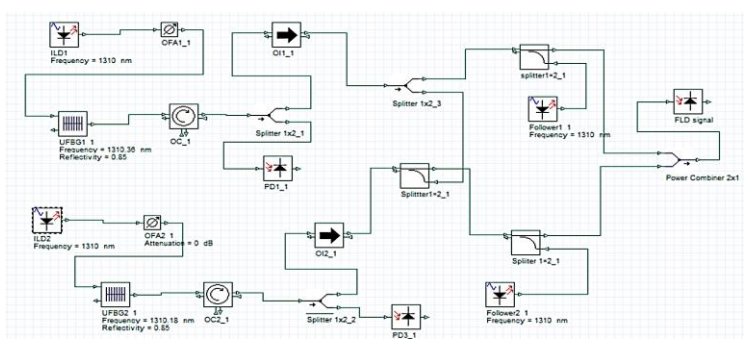


Fig.2. Experimental simulation setup of optical neural networks Drawn using Origin 2020.

3. Results and Discussions

Based on the setup, shown in Figure (2), the FLD is subjected to optical feed-forward injection from the ILD. According to this setup, ILD-MLD system dynamics are investigated for selected parameters which include: modulation optical strength.

Such a technique is designed to simulate the dynamics of an optical neural network. For all following FFTs, dynamics considered in calculations are highlighted in yellow color. For these ranges, the signal-to-noise ratio is considered high enough to track the true laser signal, i.e., the noise spectrum is excluded from calculations.

3.1. Effect of OAF1

Results for observed results; time series, FFTs, FWMH, number of peaks, attractors, and correlation coefficient, are all given in Figures 3, 4, 5, 6, and 7, respectively. Figure, part (A) represents the signals observed from the influencer laser, while (B) represent those identical signals, observed in the same individual run, for the follower laser. The variable parameter is laser bias voltage, which changed from -20dB to -45dB, with a measured threshold current of 13.65 mA, and a measured optical power of -12 dB, after OFA is -20 dB.

Time series given in part (A) time series are all it is considered unclear, although the changes in capacity over time are weak, and therefore it is not possible to judge whether it indicates chaotic behavior or not based on it alone. The degree of choice fluctuates from optical power value to another, i.e., the perturbation period time duration is changed. Especially at the value of -35dB, which gives a large change in the amplitude of the signal over time, as is clear. Differences in signal amplitude can be attributed to the effect of light reflection from OC and UFBG to influencer laser. The behavior in part (B) indicates a clear behavior of the amplitude changes of the dependent laser wave and clearly with the effective laser power, which predicts the presence of chaotic behavior, as will be observed later when analyzing the Fourier wave.

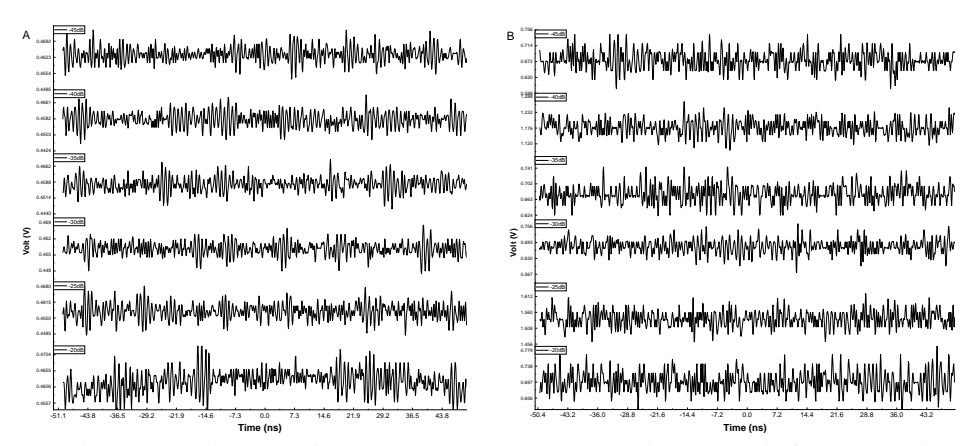


Fig. 3. Time series at various optical power attenuator1 (A) ILD1 influencer signal, (B) FLD follower signal.

In Fourier space, the last observations are given in figure (4), which shows variation in lasing mode frequency and amplitude. This means that their variable response from the follower laser to the same modulation frequency value came from a variable laser power. Due to optical chaotic modulation, there exists a possibility to synchronize the follower laser from the influencer laser. Appeared a narrow spectral in section (A) at MHz frequency and a broad spectral (B) at GHz. Narrow linewidth lasers are essential for applications such as coherent optical communication systems and microwave photonics. Typically, their linewidth is decreased by either extending the photon lifetime using an external cavity or by stabilizing the laser with advanced electronics to a stable reference. Through Optical Injection Locking (OIL), cost-effective lasers with relatively broad line widths can be transformed into high-performance, narrow linewidth lasers [37].

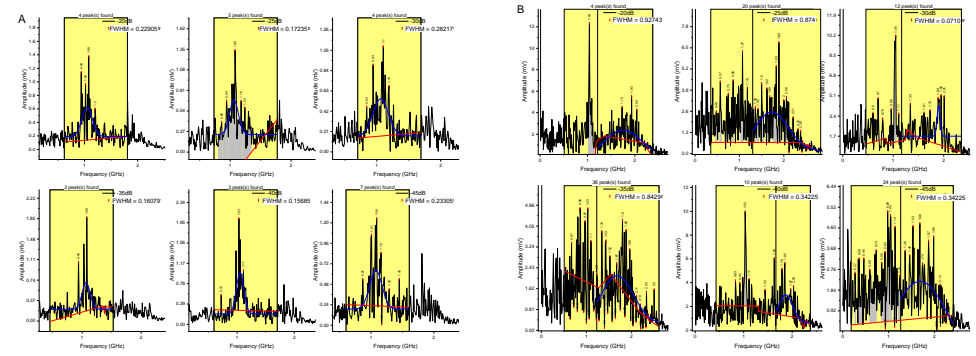


Fig. 4. The results of the FFT for the effect of the ILD1 optical power in ILD-FLD system dynamics. (A) ILD1, (B) FLD.

As shown in Figure (5), the FWHM changes with the optical power of ILD1. The change (A, B) is described by is a polynomial function. This change is described by Piecewise PWL3 functions, often used to approximate nonlinear functions, especially those with sharp corners or discontinuities, and by rational functions, which are expressed as the quotient of two polynomials and a polynomial function is a function that involves only non-negative integer powers or only positive integer exponents of a variable in an equation like the quadratic equation, or cubic equation, which are functions consisting of many algebraic terms including constants, variables of different degrees, coefficients, and positive exponents. The degree of the polynomial function is the highest exponent of the variable. The best value obtained is 0.8 GHz at -20dB (B), this is important because increasing the FWHM value of the offer contributes greatly to the communication and the modulation of the signal. The gain bandwidth is defined as the full width at half maximum (FWHM) of the gain spectrum ($\Delta v_g = \frac{\Delta w_g}{2\pi}$) [38].

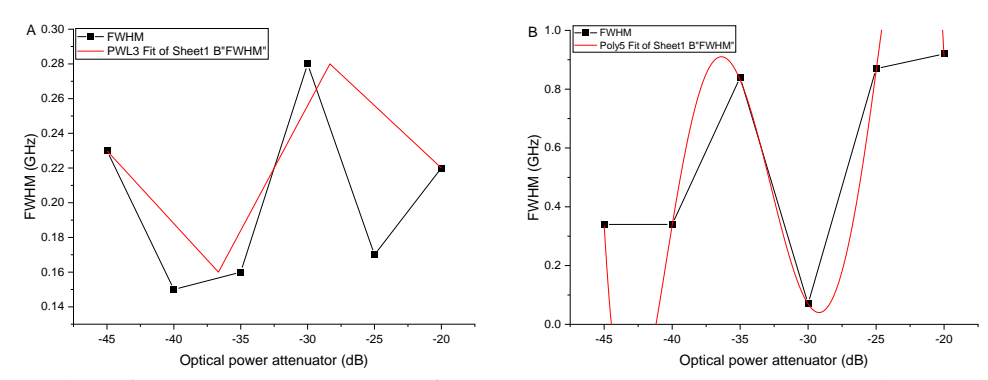


Fig. 5. Relations for measured FWHM for power laser ILD1 :(a) ILD1 (A) and (B) FLD.

Figure (6) shows the phase space of ILD1 and FLD laser attractors. An attractor is called strange if it has a fractal structure. This is often the case when the dynamics on it are chaotic, exhibiting sensitive dependence on initial conditions. It is a form of non-linear attractor, meaning that it does not follow the traditional laws of linear motion, the laser beam tends to return to the same region of space. it noted central region (A) is empty indicating a weak chaos of influencer signal, unlike (B) attractor. The transmitter signal is amplified since the receiver laser's optical power is marginally greater than the transmitter's. The lowering of the receiver laser's carrier density and optical injection-induced reduction of the laser's gain are characteristic features of the difference. As a result, perfect and generalized synchronization have entirely distinct physical origins [39].

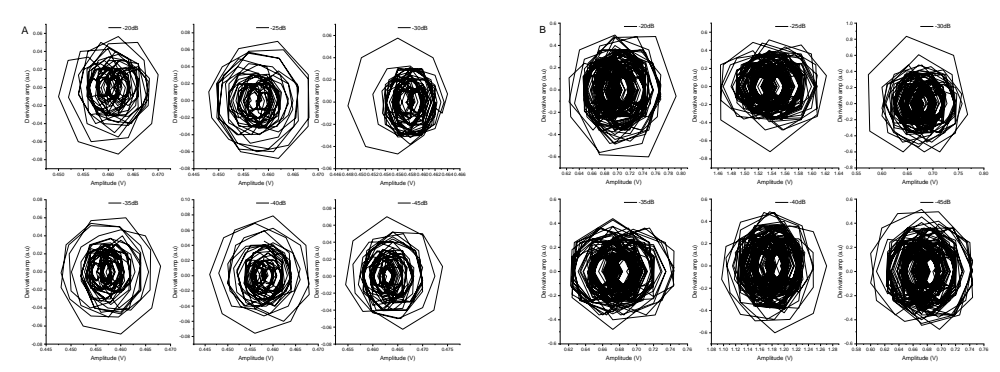


Fig. 6. The results of the phase space for the effect of the optical power ILD1 in ILD-FLD system dynamics. (A) ILD1, (B) FLD.

The correlation coefficient between both lasers is calculated and shown in Figure (7). Resulted relation is satisfied fitting by the Exponential function. According to the correlation coefficient of influencer1-follower, the correlation coefficient is positive and negative values for all ranges, which indicates the direct relationship of effect, in which the relationship is proportional universal. It is challenging to see perfect chaotic synchronization since the transmitter and receiver lasers' device settings need to match. As a result, not many experimental findings have been shared. Using comparable systems of semiconductor lasers with optical feedback, Liu et al [39, 26] reported experimental full chaotic synchronization. Complete chaos synchronization utilizing electro-optic hybrid chaos systems with semiconductor lasers was also experimentally reported by Tang et al. [41]. They demonstrated the existence of full chaotic synchronization in actual lasers by observing the time delay. The frequency detuning between the two lasers was crucial to their tests and was almost nonexistent.

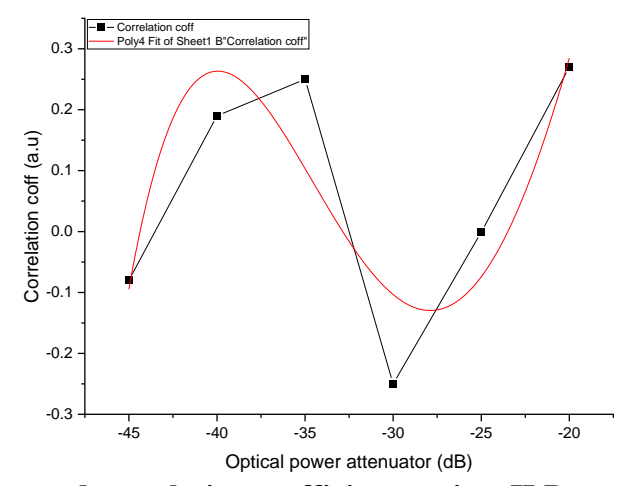


Fig. 7. Measured correlation coefficient against ILD optical power.

3.2. Effect of OAF2

Results for observed results; time series, FFTs, FWMH, attractors, and correlation coefficient, are all given in figures 8, 9, 10, 11, and 12, respectively. Figure (8), part (A) represents the signals observed from the influencer laser, while (B) represents the follower signal of laser signals. The variable parameter is laser bias voltage, which changed from -20dB to -45dB, with a measured threshold current of 13.65 mA, and a measured optical power of -12 dB, after OFA is -20 dB. Time series given in part (A) time series the perturbation period time duration is changed from the value to the next. Especially at the value of -30dB, which gives a large change in the amplitude of the signal over time, as is clear. The amplitude changes of the follower laser signal shown in (B) are observed, indicating the presence of a good chaotic signal due to the effect of the optical injection by lasers ILD2. Thus, the optical injection has shown us new dynamics in the laser, as a result of several processes occurring in the laser cavity laser.

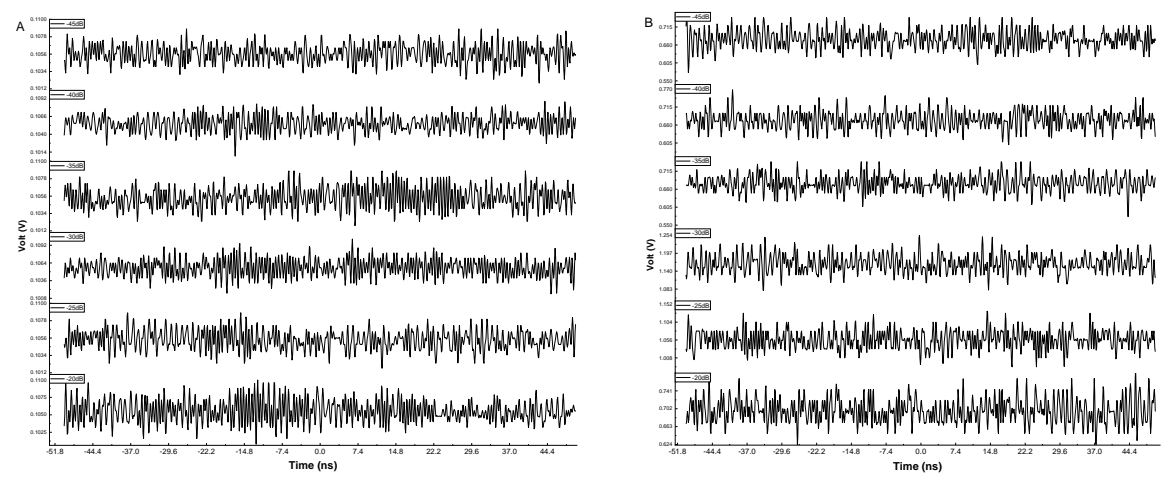


Fig. 8. Time series at various influencer ILD2 optical power (A) ILD2 influencer signal, (B) FLD follower signal.

Fourier space is considered one of the important analyses to examine the chaos of the signal, the last observations are given in Figure (9), which shows variation in lasing mode frequency and amplitude. This means that their variable response from the follower laser to the same modulation frequency value came from a variable optical power influencer. The presence of a transverse spectrum at certain values, which supports the chaotic behavior of the laser, can be attributed to several reasons, including reflections within the optical fiber and through the BRAC resolver, which play an important role in the reflected signal and the appearance of chaotic behavior in the signal, while a broad spectral (B) at GHz is due to chaos in the signal from optical injection.

The mechanisms underlying sudden chaotic transitions are homoclinic and heteroclinic tangency bifurcations. Nevertheless, the changes described here are sudden compared to situations where an attractor changes continuously with parameters during the bifurcation (as is the case, for example, for a periodic orbit disappearing in a Hopf bifurcation) [42].

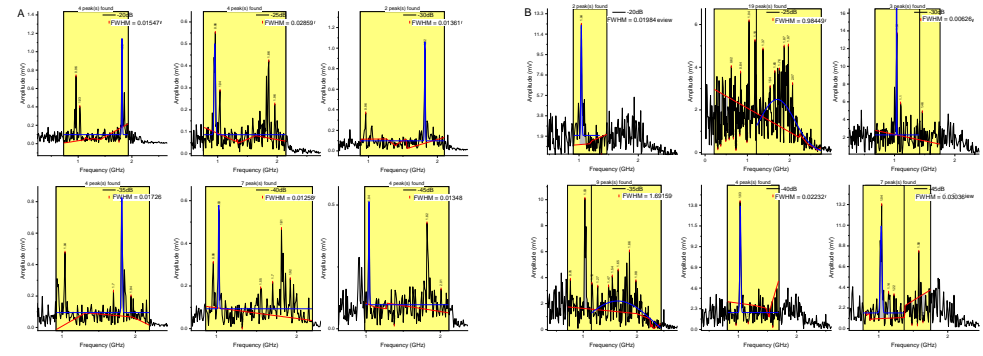
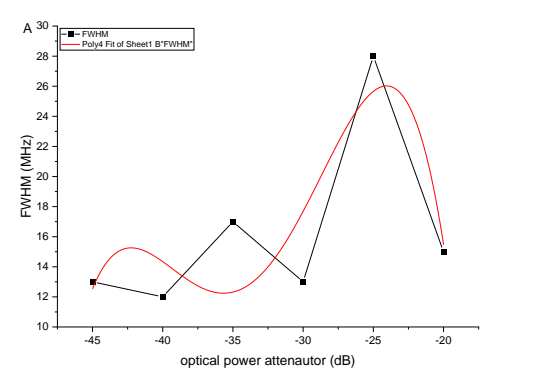


Fig. 9. The results of the FFT for the effect of the ILD2 optical power in ILD-FLD system dynamics. (A) ILD2, (B) FLD.

As shown in Figure (10), the FWHM changes with a optical power of ILD2. The change (A,B) is described by the polynomial function. The best value obtained is 1.6 GHz at -35dB (B), This value is excellent because the work is limited to a frequency range of 2GHz by the oscilloscope. Besides the broad spectral peaks of the external cavity mode and its higher harmonics, at some voltage, the laser was operating in a weak chaotic state close to a quasiperiodic oscillation. The broad peaks are very good for coded messages in chaotic signals. The interaction of the injection light with the chaotic laser field through beating results in a high-frequency oscillation, which is the physical process of bandwidth improvement by optical injection.

Higher-bandwidth chaos can be produced by a chaotic laser with dual-optical injection because it can accomplish more frequency detuning within the interaction range than a single-optical injection [43].



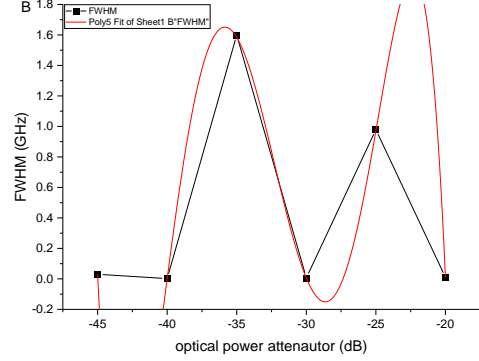


Fig. 10. Relations for measured FWHM for influencer laser optical power: (A) ILD2 and (B) FLD.

Figure (11) shows the phase space of ILD2, FLD laser attractors. An attractor is called strange if it has a fractal structure. This is often the case when the dynamics on it are chaotic, exhibiting sensitive dependence on initial conditions. It is a form of non-linear attractor, meaning that it does not follow the traditional laws of linear motion, the laser beam tends to return to the same region of space. It is easy to understand that optical injection reduces the threshold carrier in the FLD since the externally injected light provides a sufficient amount of photons to reach the threshold of the laser, both stimulated and spontaneous emission contribute to making the system into a state of chaos. The attractor diagram corresponds to FFts in Figure (9).

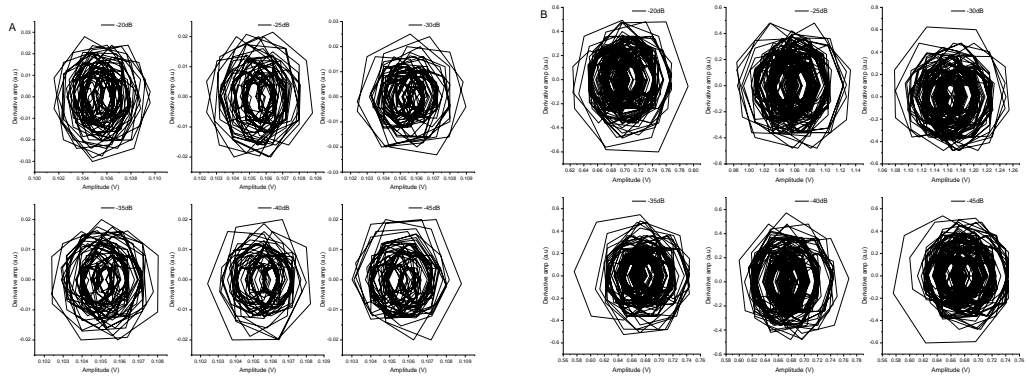


Fig. 11. The results of the phase space for the effect of the ILD optical power V in ILD-FLD system dynamics. (A) ILD2, (B) FLD.

Synchronization of chaotic systems has been given much attention due to its potential in secure communication systems. The underlying concept is that the transmitted message should be encoded within the noiselike output of a chaotic transmitter. Hence synchronization, and its dependence on various experimental parameters, are of paramount importance. The most common method of characterizing the quality of synchronization of two lasers is to plot a synchronization diagram: at each point in time the intensity of one laser is plotted as a function of the intensity of the other. If the two lasers are perfectly synchronized, the synchronization plot will be a straight line with a positive gradient. Less than perfect synchronization leads to a broadening of the plot [44]. The correlation coefficient between both lasers is calculated and shown in Figure (12). Resulted relation is satisfied fitting by polynomial function (A) ILD-FLD1, and the polynomial function ILD-FLD2. According to the correlation coefficient positive and negative values as voltage of ILD2 change. The best value it has been reached is 0.26 at -40dB (A).

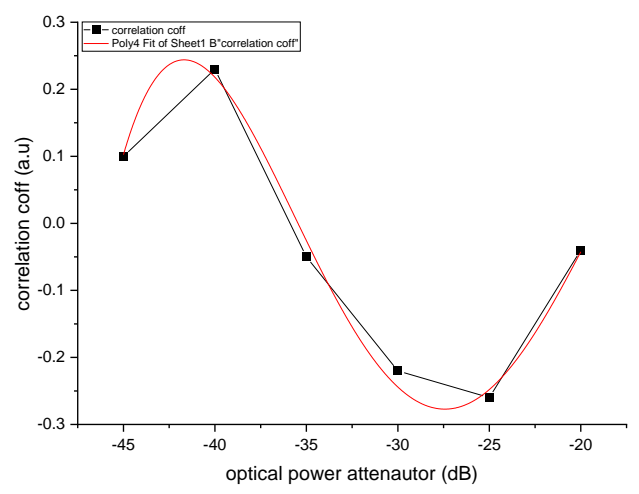


Fig. 12. Measured correlation coefficient against ILD2 optical power: (A) ILD2-FLD.

4. Conclusions

A simple chaotic circuit has been introduced and investigated through experimental implementation. Active mediums can interact chaotically with applied modulation, and the resulting dynamics are subject to this interaction. discussed and its application to secure communications has also been presented in synchronization of chaotic oscillations in semiconductor lasers with optical injection. The expected evolution for the last two initial conditions is that variation fluctuates from strange to limited circle-shaped attractors. Such a system satisfies FF dynamics in the OI version.

Acknowledgments

The authors would like to thank Mustansiriyah University, Baghdad- Iraq for their support of this research.

Reference

- [1] M. J. Weber, *Handbook of lasers*, vol. 18. CRC press, 2000.
- [2] D. Zhong *et al.*, 'Significant improvement of chaotic synchronization quality of two polarization components emitted by an optically pumped spin-VCSEL using wavelet decomposition in photonic reservoir computers', *Optics Communications*, p. 130907, 2024.
- [3] K. Kikuchi, T. Okoshi, M. Nagamatsu, and N. Henmi, 'Degradation of bit-error rate in coherent optical communications due to spectral spread of the transmitter and the local oscillator', *Journal of lightwave technology*, vol. 2, no. 6, pp. 1024–1033, 1984.
- [4] Z. Liu, J.-Y. Kim, D. S. Wu, D. J. Richardson, and R. Slavik, 'Homodyne OFDM with optical injection locking for carrier recovery', *Journal of Lightwave Technology*, vol. 33, no. 1, pp. 34–41, 2014.
- [5] J. El-Azab and M. Hemdan, 'A study of the influence of external optical injection on a semiconductor laser diode', 2013 High Capacity Optical Networks and Emerging/Enabling Technologies, HONET-CNS 2013, no. May, pp. 55–59, 2013, doi: 10.1109/HONET.2013.6729757.
- [6] Y. S. Neo, S. M. Idrus, M. F. Rahmat, S. E. Alavi, and I. S. Amiri, 'Adaptive Control for Laser Transmitter Feedforward Linearization System', *IEEE Photonics Journal*, vol. 6, no. 4, pp. 1–10, 2014, doi: 10.1109/JPHOT.2014.2335711.
- [7] Z. R. Ghayib and A. A. Hemed, 'Smart control for the chaotic dynamics using two regions uniform fiber Bragg grating', *Optoelectronics and advanced materials-Rapid communications*, vol. 16, no. July-August 2022, pp. 307–318, 2022.
- [8] T. Ismail, C. P. Liu, J. E. Mitchell, and A. J. Seeds, 'High-dynamic-range wireless-over-fiber link using feedforward linearization', *Journal of Lightwave Technology*, vol. 25, no. 11, pp. 3274–3282, 2007, doi: 10.1109/JLT.2007.906823.
- [9] A. Hemed, M. M. Fdhala, and S. M. Khorsheed, 'Modified superstructure fiber Bragg grating for a filter application', *Kuwait Journal of Science*, vol. 49, no. 1, 2022.

- [10] D. Zhang and Z. Tan, 'A Review of Optical Neural Networks', *Applied Sciences (Switzerland)*, vol. 12, no. 11, 2022, doi: 10.3390/app12115338.
- [11] H. R. Shakir, S. A. Mehdi, and A. A. Hattab, 'A New Method for Color Image Encryption Using Chaotic System and DNA Encoding', *Mustansiriyah journal of pure and Applied Sciences*, vol. 1, no. 1, pp. 68–79, 2023.
- [12] W. B. Yu and T. T. Ma, 'A study on offline handwritten Chinese character recognition based on chaotic iteration', vol. 2, no. 1, pp. 62–75, 2024.
- [13] E. Cohen, D. Malka, A. Shemer, A. Shahmoon, Z. Zalevsky, and M. London, 'Neural networks within multi-core optic fibers', *Scientific reports*, vol. 6, no. 1, p. 29080, 2016.
- [14] D. H. Nguyen and B. Widrow, 'Neural networks for self-learning control systems', *IEEE Control systems magazine*, vol. 10, no. 3, pp. 18–23, 1990.
- [15] D. R. Madhloom, A. A. Hemed, and S. M. Khorsheed, 'Experimental Simulation for Two Optically Filtered Modulation Weights in Laser Diode As a Self-Learning Layer', *East European Journal of Physics*, vol. 2023, no. 2, pp. 267–276, 2023, doi: 10.26565/2312-4334-2023-2-30.
- [16] F. P. Sunny, E. Taheri, M. Nikdast, and S. Pasricha, 'A Survey on Silicon Photonics for Deep Learning', *ACM Journal on Emerging Technologies in Computing Systems*, vol. 17, no. 4, 2021, doi: 10.1145/3459009.
- [17] F. Wu, H. Gu, and Y. Li, 'Inhibitory electromagnetic induction current induces enhancement instead of reduction of neural bursting activities', *Communications in Nonlinear Science and Numerical Simulation*, vol. 79, p. 104924, 2019.
- [18] F. Wu and H. Gu, 'Bifurcations of negative responses to positive feedback current mediated by memristor in a neuron model with bursting patterns', *International Journal of Bifurcation and Chaos*, vol. 30, no. 04, p. 2030009, 2020.
- [19] J. Zhang and X. Liao, 'Synchronization and chaos in coupled memristor-based FitzHugh-Nagumo circuits with memristor synapse', *Aeu-international journal of electronics and communications*, vol. 75, pp. 82–90, 2017.
- [20] F. Xu, J. Zhang, T. Fang, S. Huang, and M. Wang, 'Synchronous dynamics in neural system coupled with memristive synapse', *Nonlinear Dynamics*, vol. 92, no. 3, pp. 1395–1402, 2018, doi: 10.1007/s11071-018-4134-0.
- [21] M. Lv, J. Ma, Y. Yao, and F. Alzahrani, 'Synchronization and wave propagation in neuronal network under field coupling', *Science China Technological Sciences*, vol. 62, pp. 448–457, 2019.
- [22] M. E. Yamakou, 'Chaotic synchronization of memristive neurons: Lyapunov function versus Hamilton function', *Nonlinear Dynamics*, vol. 101, no. 1, pp. 487–500, 2020, doi: 10.1007/s11071-020-05715-2.
- [23] H. Lin, C. Wang, Q. Deng, C. Xu, Z. Deng, and C. Zhou, 'Review on chaotic dynamics of memristive neuron and neural network', *Nonlinear Dynamics*, vol. 106, no. 1, pp. 959–973, 2021, doi: 10.1007/s11071-021-06853-x.
- [24] H. Lin and C. Wang, 'Influences of electromagnetic radiation distribution on chaotic dynamics of a neural network', *Applied Mathematics and Computation*, vol. 369, no. March, 2020, doi: 10.1016/j.amc.2019.124840.
- [25] V. T. Pham, S. Jafari, S. Vaidyanathan, C. Volos, and X. Wang, 'A novel memristive neural network with hidden attractors and its circuitry implementation', *Science China Technological Sciences*, vol. 59, pp. 358–363, 2016.
- [26] Z. T. Njitacke, I. S. Doubla, S. Mabekou, and J. Kengne, 'Hidden electrical activity of two neurons connected with an asymmetric electric coupling subject to electromagnetic induction: Coexistence of patterns and its analog implementation', *Chaos, Solitons & Fractals*, vol. 137, p. 109785, 2020.
- [27] Y. Yu, M. Shi, H. Kang, M. Chen, and B. Bao, 'Hidden dynamics in a fractional-order memristive Hindmarsh–Rose model', *Nonlinear Dynamics*, vol. 100, pp. 891–906, 2020.
- [28] Z. Tabekoueng Njitacke, C. Laura Matze, M. Fouodji Tsotsop, and J. Kengne, 'Remerging feigenbaum trees, coexisting behaviors and bursting oscillations in a novel 3D generalized Hopfield neural network', *Neural Processing Letters*, vol. 52, no. 1, pp. 267–289, 2020.

- [29] B. Bao, H. Qian, Q. Xu, M. Chen, J. Wang, and Y. Yu, 'Coexisting behaviors of asymmetric attractors in hyperbolic-type memristor based Hopfield neural network', *Frontiers in Computational Neuroscience*, vol. 11, p. 81, 2017.
- [30] H. Lin, C. Wang, W. Yao, and Y. Tan, 'Chaotic dynamics in a neural network with different types of external stimuli', *Communications in Nonlinear Science and Numerical Simulation*, vol. 90, p. 105390, 2020.
- [31] S. Zhang, J. Zheng, X. Wang, Z. Zeng, and S. He, 'Initial offset boosting coexisting attractors in memristive multi-double-scroll Hopfield neural network', *Nonlinear Dynamics*, vol. 102, pp. 2821–2841, 2020.
- [32] Z. Li, H. Zhou, M. Wang, and M. Ma, 'Coexisting firing patterns and phase synchronization in locally active memristor coupled neurons with HR and FN models', *Nonlinear Dynamics*, vol. 104, pp. 1455–1473, 2021.
- [33] B. Xu, H. Lin, and G. Wang, 'Hidden Multistability in a Memristor-Based Cellular Neural Network', *Advances in Mathematical Physics*, vol. 2020, no. 1, p. 9708649, 2020.
- [34] H. Lin, C. Wang, Q. Hong, and Y. Sun, 'A multi-stable memristor and its application in a neural network', *IEEE Transactions on Circuits and Systems II: Express Briefs*, vol. 67, no. 12, pp. 3472–3476, 2020.
- [35] H. Bao, W. Liu, and M. Chen, 'Hidden extreme multistability and dimensionality reduction analysis for an improved non-autonomous memristive FitzHugh–Nagumo circuit', *Nonlinear Dynamics*, vol. 96, pp. 1879–1894, 2019.
- [36] C. Xiu, R. Zhou, and Y. Liu, 'New chaotic memristive cellular neural network and its application in secure communication system', *Chaos, Solitons & Fractals*, vol. 141, p. 110316, 2020.
- [37] Z. Liu and R. Slavik, 'Optical Injection Locking: From Principle to Applications', *Journal of Lightwave Technology*, vol. 38, no. 1, pp. 43–59, 2020, doi: 10.1109/JLT.2019.2945718.
- [38] G. P. Agrawal, 'Nonlinear fiber optics', in *Nonlinear Science at the Dawn of the 21st Century*, Springer, 2000, pp. 195–211.
- [39] J. Ohtsubo, 'Chaos synchronization and chaotic signal masking in semiconductor lasers with optical feedback', *IEEE Journal of Quantum Electronics*, vol. 38, no. 9, pp. 1141–1154, 2002, doi: 10.1109/JQE.2002.801883.
- [40] Y. Liu, Y. Takiguchi, P. Davis, T. Aida, S. Saito, and J. M. Liu, 'Experimental observation of complete chaos synchronization in semiconductor lasers', *Applied Physics Letters*, vol. 80, no. 23, pp. 4306–4308, 2002.
- [41] S. Tang and J. M. Liu, 'Synchronization of high-frequency chaotic optical pulses', *Optics letters*, vol. 26, no. 9, pp. 596–598, 2001.
- [42] S. Wieczorek, B. Krauskopf, T. B. Simpson, and D. Lenstra, 'The dynamical complexity of optically injected semiconductor lasers', *Physics Reports*, vol. 416, no. 1–2, pp. 1–128, 2005, doi: 10.1016/j.physrep.2005.06.003.
- [43] M. Zhang and Y. Wang, 'Review on Chaotic Lasers and Measurement Applications', *Journal of Lightwave Technology*, vol. 39, no. 12, pp. 3711–3723, 2021, doi: 10.1109/JLT.2020.3043829.
- [44] S. Sivaprakasam, I. Pierce, P. Rees, P. S. Spencer, K. A. Shore, and A. Valle, 'Inverse synchronization in semiconductor laser diodes', *Physical Review A Atomic, Molecular, and Optical Physics*, vol. 64, no. 1, p. 8, 2001, doi: 10.1103/PhysRevA.64.013805.